



Original Paper

Preparation of EVAM-g-NSiO₂ nanocomposite pour point depressant and its effect on rheological properties of model waxy oil

Yi-Hai Yang^a, Li-Na Zhang^a, Zheng-Nan Sun^{a,*}, Ming-Xing Bai^b, Guo-Lin Jing^{a,**},
Yang Liu^a, Xiao-Yan Liu^c

^a Provincial Key Laboratory of Oil □ Gas Chemical Technology, College of Chemistry □ Chemical Engineering, Northeast Petroleum University, Daqing, 163318, Heilongjiang, China

^b School of Petroleum Engineering, Northeast Petroleum University, Daqing, 163318, Heilongjiang, China

^c School of Mechanical Science and Engineering, Northeast Petroleum University, Daqing, 163318, Heilongjiang, China

ARTICLE INFO

Article history:

Received 19 February 2024

Received in revised form

7 June 2024

Accepted 19 June 2024

Available online 21 June 2024

Edited by Min Li

Keywords:

Model waxy oil

Nanoparticle

Pour point depressant

Rheological properties

Microstructure

ABSTRACT

Modified ethylene-vinyl acetate copolymer (EVAM) and amino-functionalized nano-silica (NSiO₂) particles were employed as the base materials for the synthesis of the nanocomposite pour point depressant designated as EVAM-g-NSiO₂. This synthesis involved a chemical grafting process within a solution system, followed by a structural characterization. Moreover, combining macro-rheological performance with microscopic structure observation, the influence of the nanocomposite pour point depressant on the rheological properties of the model waxy oil system was investigated. The results indicate that when the mass ratio of NSiO₂ to EVAM is 1:100, the prepared EVAM-g-NSiO₂ nanocomposite pour point depressant exhibits excellent pour point reduction and viscosity reduction properties. Moreover, the nanocomposite pour point depressant obtained through a chemical grafting reaction demonstrates structural stability (the bonding between the polymer and nanoparticles is stable). The pour points of model waxy oils doped with 500 mg/kg ethylene-vinyl acetate copolymer (EVA), EVAM, and EVAM/SiO₂ were reduced from 34 °C to 23, 20, and 21 °C, respectively. After adding the same dosage of EVAM-g-NSiO₂ nanocomposite pour point depressant, the pour point of the model wax oil decreased to 12 °C and the viscosity at 32 °C decreased from 2399 to 2396.9 mPa · s, achieving an impressive viscosity reduction rate of 99.9%. Its performance surpassed that of EVA, EVAM, and EVAM/SiO₂. The EVAM-g-NSiO₂ dispersed in the oil phase acts as the crystallization nucleus for wax crystals, resulting in a dense structure of wax crystals. The compact wax crystal blocks are difficult to overlap with each other, preventing the formation of a three-dimensional network structure, thereby improving the low-temperature flowability of the model waxy oil.

© 2024 The Authors. Publishing services by Elsevier B.V. on behalf of KeAi Communications Co. Ltd. This is an open access article under the CC BY-NC-ND license (<http://creativecommons.org/licenses/by-nc-nd/4.0/>).

Abbreviations

WAT	wax appearance temperature
FIs	flow improvers
PPDs	pour point depressants
EVA	ethylene-vinyl acetate copolymer
POA	polyoctadecyl acrylate
NSiO ₂	amino-functionalized nano-silica
EVAM	(EVA-maleic anhydride) copolymer
MAH	maleic anhydride
APTS	3-aminopropyltriethoxysilane
SiO ₂	inorganic nano-silica
YSiO ₂	organic modification on nano-silica
GO	graphene oxide
PMMA	poly(methyl methacrylate)
P(2EHA)	poly(2-ethylhexyl acrylate)
AIBN	azobisisobutyronitrile

* Corresponding author.

** Corresponding author.

E-mail addresses: sunzhengnan@nepu.edu.cn (Z.-N. Sun), jglxueshu@yeah.net (G.-L. Jing).

1. Introduction

Waxy crude oil contains a significant amount of paraffin molecules with a carbon atom number ranging from C_{16} to C_{40} . In the course of transporting waxy crude oil through pipelines, paraffin molecules initiate crystallization and precipitation when the temperature drops below the wax appearance temperature (WAT) due to oversaturation (Liu et al., 2023; Valinejad and Nazar, 2013; Yao et al., 2016a). In the petroleum industry, wax deposition poses a complex and costly challenge as the precipitation of wax complicates the low-temperature flow characteristics of oil within transportation pipelines (Azevedo and Teixeira, 2003; Yang et al., 2015b). Alternatively, when the pipeline wall temperature is slightly below the WAT, it encourages the deposition of wax molecule layers. Over time, the growth of these layers of wax molecules adversely impacts the performance of the pipeline (Pedersen and Rønningsen, 2003). Especially in colder regions, addressing wax deposition issues is crucial due to the heightened risk of severe wax precipitation in large-scale petroleum production (Aiyejina et al., 2011).

Utilizing chemical additives, such as flow improvers (FIs) and pour point depressants (PPDs), has emerged as a recognized and effective method for addressing these issues (Ghosh and Das, 2014; Ghosh et al., 2017; Yang et al., 2023). PPDs/FIs in waxy crude oil primarily function through nucleation, adsorption, and eutectic alteration to modify crystal growth habits, effectively preventing the interconnection of wax crystals (Al-Sabagh et al., 2017; Alves et al., 2023; Fang et al., 2012). Hence, the incorporation of PPDs/FIs markedly decreases both the pour point and viscosity of waxy crude oil.

Ethylene-vinyl acetate copolymer (EVA) and its modified derivatives are presently the most extensively utilized commercial PPDs (Ruwoldt et al., 2017; Wei, 2015; Yang et al., 2015b). EVA and its copolymers with maleic anhydride have been thoroughly investigated as PPDs for waxy crude oil (Steckel et al., 2022; Umoruddin et al., 2019). Previous studies have clarified the influence of polar groups, their content, molecular weight, and oil phase composition on the efficacy of PPDs of the EVA type (Yao et al., 2018).

In recent years, the research prospects for polymer/nanocomposite materials have become increasingly compelling. This novel material can serve as a cost-effective alternative to high-performance composite materials for researchers across diverse industries (Paul and Robeson, 2008; Schmidt et al., 2002). Taking inspiration from the outstanding performance of polymer/inorganic nanocomposite materials, diverse types of inorganic nanoparticles have recently been incorporated into conventional polymer PPDs to create nanocomposite PPDs. Through the meticulous blending of nanomaterials, including nano-silica, nano-clay, and graphene oxide, with polymer PPDs, diverse types of nanocomposite PPDs have been successfully synthesized (Jia et al., 2022; Jing et al., 2017; Liu et al., 2021; Yao et al., 2016b). Yang et al. (2015a) and Norrman et al. (2016) added polyoctadecyl acrylate (POA) and an equal mass of inorganic nano-silica (SiO_2) to a toluene solution, producing hybrid particles of POA/ SiO_2 through ultrasonic treatment and vigorous stirring. The results indicate that the produced PPDs effectively reduce the gelation point and yield stress of the model waxy oil. However, not all SiO_2 particles are entirely coated by POA, and these SiO_2 particles act as additional suspended particles, increasing viscosity. Zhao et al. (2017) prepared nanohybrid PPDs by covering organic modified nano-clay in polymeric PPDs. The results indicate that, compared to polymer PPDs, nanohybrid PPDs consistently exhibit superior performance. Among them, the nanohybrid PPD with a mass ratio of polymer PPD to organically modified nano-clay of 4:1 shows the best pour point reduction effect. Zhang et al. (2020) conducted a hybrid study using SiO_2 and

benzyl methacrylate-methacrylate copolymers (MB- R_1 MC), investigating the impact of nano- SiO_2 /MB- R_1 MC on the low-temperature flow performance of diesel. The results indicate that, at the same dosage, the inhibitory effect of nano- SiO_2 /MB- R_1 MC on diesel is superior to MB- R_1 MC alone. The optimal performance is achieved at a mass ratio of 1:6 for nano-silica/MB- R_1 MC. Sun et al. (2018) initially performed organic modification on nano-silica ($YSiO_2$) and subsequently crafted $YSiO_2$ /EVA PPD (the mass ratio between $YSiO_2$ and EVA is 1:1) through the chemical grafting of EVA with the $YSiO_2$ using a solution polymerization method. The results demonstrated that the $YSiO_2$ enhanced compatibility with EVA. Compared to pure EVA, the nanocomposite PPDs exhibited a substantial improvement in the flowability of waxy crude oil. Yang et al. (2017) demonstrated through adsorption experiments that EVA molecules can adsorb onto polymethylsilsesquioxane (PMSQ) microspheres, forming EVA/PMSQ composite particles. When the mass ratio of EVA to PMSQ is 100:5, the composite particles can serve as nucleation templates for wax precipitation, resulting in larger and denser wax microstructures, thereby effectively improving the flowability of the oil. In subsequent experiments, they subjected the PMSQ microspheres to amino-functionalization modification and named them PAMSQ (Yao et al., 2018). Compared to PASQ, PAMSQ microspheres are more conducive to the adsorption and concentration of more EVA PPDs on the microspheres. Compared to EVA/PMSQ, EVA/PAMSQ exhibits stronger nucleation effects. Sharma et al. (2019b) synthesized polymer nanocomposite material poly(methyl methacrylate)-graphene oxide (PMMA-GO) using graphene oxide (GO) and poly(methyl methacrylate) (PMMA). The results indicate that the addition of only 1 wt% of graphene oxide (GO) in the nanocomposite pour point depressant significantly reduces the pour point and viscosity of crude oil. Sharma et al. (2019a) successfully synthesized a novel polymer nanocomposite material, P(2EHA)-GO (poly(2-ethylhexyl acrylate)-GO), in the laboratory. Among them, P(2-EHA)-1%GO demonstrated better wax inhibition performance compared to the P(2-EHA) (poly(2-ethylhexyl acrylate)) polymer PPD. It not only significantly reduced the pour point of crude oil but also endowed the crude oil with excellent restart flowability. In conclusion, the observations are as follows: (a) All prepared nanocomposite PPDs demonstrate effective performance in reducing pour point and viscosity. (b) Organic modification of inorganic nano-silica/nano-clay enhances compatibility with polymer PPDs. While nanocomposite pour point depressants were successfully prepared, the usage of nanoparticles was relatively high. (c) Utilizing carbon nanomaterials not only significantly reduces the content of nanoparticles in the nanocomposite pour point depressant but also greatly enhances the effectiveness of the nanocomposite pour point depressant. (d) However, carbon nanomaterials are expensive, making it challenging for widespread industrial applications. Therefore, the organic modification of inorganic nanoparticles is a worthwhile and in-depth research direction.

This study involved the preparation of amino-functionalized nano-silica ($NSiO_2$) through the organic modification of SiO_2 . Simultaneously, (EVA-maleic anhydride) copolymer (EVAM) was synthesized using solution graft copolymerization. Following this, through chemical grafting, EVAM-g- $NSiO_2$ nanocomposite PPD was successfully prepared under the condition where the dosage of $NSiO_2$ was only 1 wt% of EVAM (i.e., a mass ratio of 1:100). According to existing research, only when the nanoparticles are carbon-based nanomaterials (such as graphene oxide) can the content of nanoparticles be so low. To visually observe the interaction between the PPD and wax, this study prepared model waxy oil with a wax content of 20 wt% to evaluate the performance of the EVAM-g- $NSiO_2$ nanocomposite PPD. The impact of EVAM, EVAM/ SiO_2 , and EVAM-g- $NSiO_2$ nanocomposite PPDs on the flow

properties of a model waxy oil was investigated through viscosity tests and microscopic observations.

2. Experiment

2.1. Materials

Materials utilized in this study included EVA (VA = 33, Melt Flow Rate = 43 g/10 min), Azobisisobutyronitrile (AIBN), Toluene, Methanol, Maleic Anhydride (MAH), 3-Aminopropyltriethoxysilane (APTS), Inorganic nano-silica (SiO₂, average particle size 30 nm) obtained from Shanghai Aladdin Biochemical Technology Co., Ltd., Shanghai. –35[#] Diesel and 58[#] Paraffin were provided by Daqing Petrochemical Company. The carbon number distribution of –35[#] diesel oil and model waxy oil is shown in Fig. 1.

2.2. Sample preparation

2.2.1. Preparation of model waxy oil

Paraffin supplied by Daqing Petrochemical Company was dissolved in diesel and stirred for 2 h at 60 °C, resulting in a model oil system with a 20 wt% wax content. The physical characteristics of model waxy oil are listed in Table 1.

2.2.2. Preparation of EVAM

A mass of EVA and MAH ($m_{\text{EVA}}:m_{\text{MAH}} = 1:3, 1:4, 1:5, 1:6, 1:7$) was dissolved in toluene with AIBN as the initiator (0.1, 0.2, 0.3, 0.4, 0.5 wt%), and nitrogen was continuously vented for 0.5 h during stirring. The reaction solution gradually changes from a colorless transparent solution to a yellow solution during this period. The copolymer was precipitated and filtered in excess cold methanol solution, then residual solvent was removed in a vacuum drying oven at 60 °C to obtain EVAM precipitant.

2.2.3. Preparation of NSiO₂

The screening process for the preparation of NSiO₂ is presented in the Supplementary Materials, and the optimal preparation conditions are as follows: At 30 °C, a specific quantity of APTS (a mass ratio of 100:5 between SiO₂ and APTS) was evenly distributed in an ethanol-water solution (with an ethanol-to-water ratio of 9:1). In the presence of ultrasonic waves and mechanical stirring, the substance underwent thorough dispersion and hydrolysis. Following a 1.5 h duration of this procedure, SiO₂ nanoparticles were introduced into the solution, and the temperature was elevated to 70 °C for an additional 3 h of stirring. After the reaction, the mixture underwent centrifugation, and the resulting product was thoroughly washed with ethanol and deionized water. Organically modified SiO₂ was obtained after vacuum drying the

Table 1
Physical characteristics of model waxy oil.

Wax, wt%	Pour point, °C	ρ_{20} , g/cm ³	50 °C Kinematic viscosity, mm ² /s
20	34	0.818	2.77

product for 12 h. The resulting product is denoted as NSiO₂.

2.2.4. Preparation of nanocomposite PPDs

The preparation steps for the EVAM/SiO₂ nanocomposite PPD are as follows: EVAM and SiO₂ are introduced into a toluene solvent at 70 °C, and they undergo thorough mixing with the assistance of ultrasonication and mechanical stirring. After the completion of the reaction, the excess solvent was removed using a rotary evaporator, followed by repeated washing of the product with cold methanol solution. Following this, it is vacuum-dried for 12 h to obtain the EVAM/SiO₂ nanocomposite PPD.

The synthesis steps for the EVAM-g-NSiO₂ nanocomposite PPD are as follows: A specific amount of EVAM and NSiO₂ is introduced into a toluene solvent at 70 °C. They undergo thorough mixing for 2 h with the aid of ultrasonication and mechanical stirring to facilitate the acylation reaction for chemical grafting. The surplus solvent is eliminated using a rotary evaporator, and the resulting product undergoes repeated washing with cold methanol solution. Subsequently, it undergoes vacuum drying for 12 h to obtain the EVAM-g-NSiO₂ nanocomposite PPD.

2.3. Proton nuclear magnetic resonance (¹H NMR)

The ¹H NMR measurements were conducted using an AVANCE III 500 (Bruker, Germany), with tetramethylsilane (TMS) as the reference standard and deuterated chloroform (CDCl₃) as the solvent.

2.4. Fourier transform infrared spectroscopy (FTIR)

The analysis was conducted using an FTIR, model TENSOR 27, from Bruker, Germany. Samples were pressed with potassium bromide (KBr) into pellets for characterization of the components of APTS, SiO₂, NSiO₂, and EVAM-g-NSiO₂.

2.5. Thermogravimetry (TGA)

The TGA was performed using an HTG-1 instrument (Beijing Hengjiu Experimental Equipment Co., Ltd.). The analysis was conducted in a nitrogen environment with a flow rate of 50 mL/min, and the temperature was increased from 0 to 800 °C at a rate of 10 °C/min.

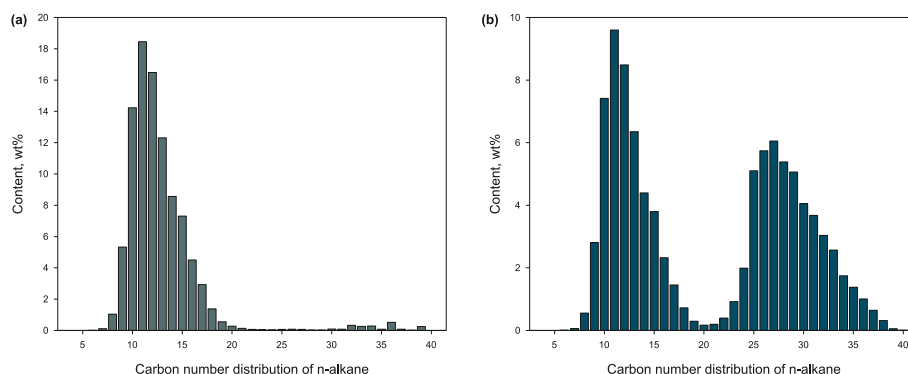


Fig. 1. Carbon number distribution of (a) –35[#] diesel oil and (b) model waxy oil.

2.6. Pour point measurement

The pour points of the undoped/doped model waxy oil were measured on the basis of the method given in the standard ASTM D97-17a method. Heat the oil sample in a water bath to make it flow. Then pour the oil sample into a test tube to the mark, and insert the thermometer fitted in a cork stopper into it. The test tube is placed in an ice water bath. As the temperature decreases, the fluidity of the oil sample is observed until the pour point is determined. Each oil sample was tested in triplicate to ensure the validity of parallel experimental data, with uncertainty bars provided in the corresponding figures.

2.7. Rheological measurement of model waxy oil

The viscosity of the model waxy oil undoped and doped with PPDs was measured using a Brookfield DV-II + Pro rotational viscometer (manufactured by Brookfield, USA) equipped with a heating and cooling system. The oil sample was cooled from 60 to 20 °C at a rate of 1 °C/min for measurement. The shear rate was fixed at 20 s⁻¹. The viscosity values at different temperatures during this cooling process were recorded.

2.8. Microscopic observation of model waxy oil

A polarizing optical microscope (POM), ZEISS AXIO Lab.1 model (Germany), was used to observe the wax crystal morphology in the model waxy oil without and with the addition of PPDs. The samples were observed after cooling from 60 to 20 °C at a rate of 1 °C/min.

3. Results and discussion

3.1. Screening of synthesis conditions for EVAM-g-NSiO₂ nanocomposite PPDs

(1) Effect on Pour Point

Fig. 2 illustrates the influence of the prepared nanocomposite PPDs on the pour point of the oil samples. Fig. 2 reveals that nanocomposite PPDs synthesized under various monomer ratio

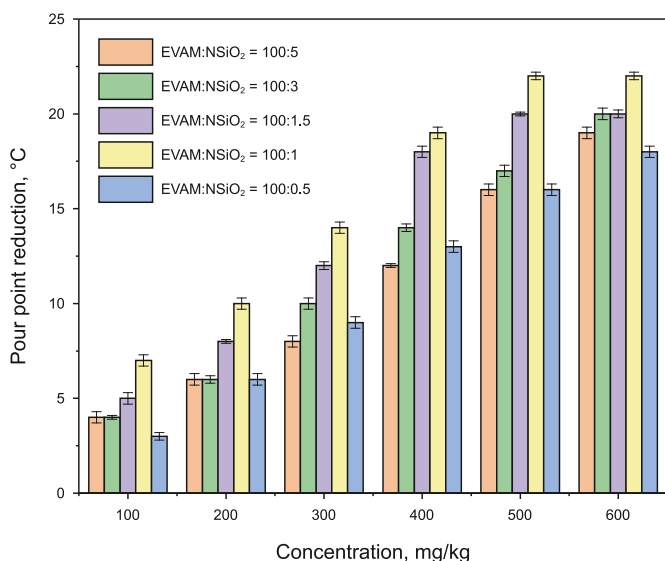


Fig. 2. The impact of different mass ratios of EVAM and NSiO₂ on the pour point of the prepared EVAM-g-NSiO₂ nanocomposite PPDs.

conditions exert a significant influence on the pour point of waxy oil samples. As the mass fraction of NSiO₂ increases, the PPDs effect exhibits an initial increase followed by a decrease. The EVAM-g-NSiO₂ nanocomposite PPD, synthesized with a mass ratio of 100:1 between EVAM and NSiO₂, exhibits the most effective depressant effect at a concentration of 500 mg/kg. Under these conditions, the pour point decreased to 12 °C, representing a reduction of 22 °C compared to the undoped oil sample.

(2) Effect on Viscosity

When doped with 500 mg/kg, the impact of various nanocomposite PPDs on the viscosity of oil samples is illustrated in Fig. 3. As observed in Fig. 3, the introduction of nanocomposite PPDs, synthesized by varying monomer ratios, led to a decrease in the viscosity of the oil samples. The viscosity of undoped oil samples exhibited a significant surge at 35 °C, reaching 2399 mPa·s as the temperature decreased to 32 °C. In contrast, oil samples doped with nanocomposite PPDs displayed minimal fluctuations in viscosity at temperatures exceeding 30 °C. Fig. 3 illustrates that the most significant reduction in viscosity was attained with the EVAM-g-NSiO₂ nanocomposite PPD synthesized at a mass ratio of 100:1 between EVAM and NSiO₂, corroborating the findings of the pour point tests.

In summary, when the mass ratio of EVAM to NSiO₂ is 100:1, the prepared EVAM-g-NSiO₂ nanocomposite PPD exhibits optimal pour point and viscosity reduction effects on model waxy oil. Therefore, the EVAM-g-NSiO₂ nanocomposite PPDs used in subsequent experiments are all prepared at this ratio.

3.2. Characterization of NSiO₂ and EVAM-g-NSiO₂ nanocomposite PPD

Fig. 4 shows the ¹H NMR spectra of EVA and EVAM PPDs. From Fig. 4(b), a new characteristic peak appears at δ = 3.69, which is the H peak on the five-membered ring after the MAH double bond is opened and connected to the EVA side chain. Combining the data from the FTIR spectrum, it can be concluded that the double bond in MAH has been successfully opened and grafted onto EVA, providing evidence for the polymerization reaction.

Fig. 5 illustrates the FTIR spectra of APTS, SiO₂, NSiO₂, and

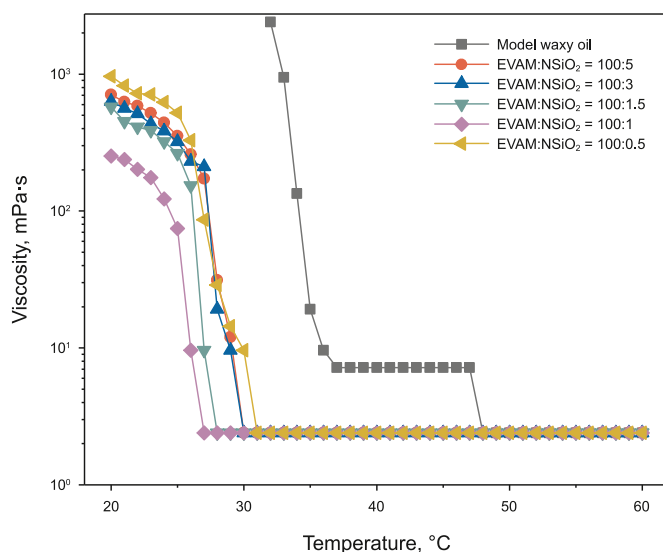


Fig. 3. Viscosity of model waxy oil doped with different monomer ratios of nanocomposite PPDs at 500 mg/kg.

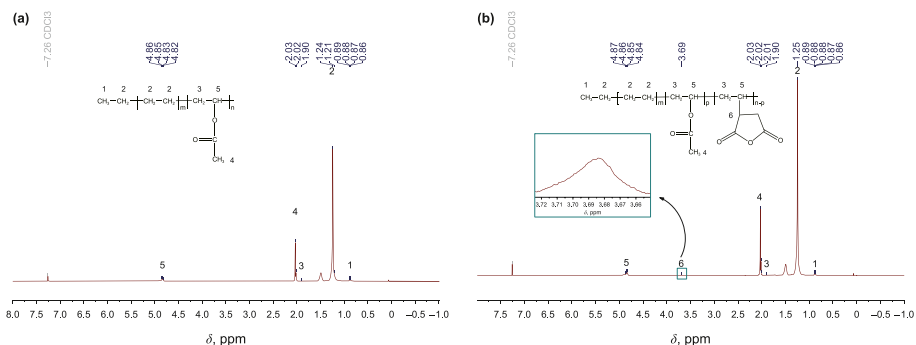


Fig. 4. ¹H NMR spectra and corresponding structures of (a) EVA and (b) EVAM.

EVAM-g-NSiO₂ nanocomposite PPDs. The FTIR spectrum of SiO₂ displays stretching vibration peaks at 3440 cm⁻¹, corresponding to the –OH bond, a bending vibration absorption peak at 1646 cm⁻¹ resulting from the H–O–H structure, an asymmetric vibration absorption peak at 1103 cm⁻¹ attributed to the Si–O–Si group, and a symmetric vibration absorption peak at 469 cm⁻¹ associated with the Si–O–Si group. Following APTS modification, NSiO₂ exhibits new absorption peaks at 2928 and 2877 cm⁻¹, representing the asymmetric and symmetric stretching vibrations of the C–H bond, affirming the presence of –CH₂ groups in NSiO₂. Peaks at 3442 and 1628 cm⁻¹ indicate N–H stretching and bending vibrations, confirming the successful modification of the SiO₂ surface by APTS. In the FTIR spectrum of EVAM-g-NSiO₂ nanocomposite material, new absorption peaks at 2928 and 2855 cm⁻¹, associated with the asymmetric and symmetric stretching vibrations of the C–H bond, verify the presence of –CH₂ groups in the nanocomposite material. Peaks at 1112 and 469 cm⁻¹ represent asymmetric and symmetric vibrations of the Si–O–Si group. Peaks at 3456 and 1656 cm⁻¹ exhibit N–H and C=O stretching vibrations related to the amide group, demonstrating the presence of the amide group in the product (Elbanna et al., 2017). This confirms the successful synthesis of EVAM-g-NSiO₂ nanocomposite material.

3.3. Thermogravimetry (TGA)

The TGA curves of EVAM/SiO₂ and EVAM-g-NSiO₂ under a nitrogen atmosphere are presented in Fig. 6. The graph indicates a noticeable weight loss starting around 110 °C, attributed to the evaporation of moisture in the sample during heating. A second significant weight loss commences at approximately 270 °C, primarily associated with the decomposition of the vinyl acetate side chain and certain unstable oxygen-containing groups (Liu et al., 2021; Silviya et al., 2012). A third distinct weight loss occurs around 400 °C, resulting from the thermal decomposition of organic molecular chains. It is noteworthy that the weight loss for EVAM/SiO₂ is 89.79 wt%, indicating that the interaction between SiO₂ and EVAM involves simple physical adsorption. During the preparation of EVAM/SiO₂ through solution blending, EVAM is not entirely coated on the surface of SiO₂. Simultaneously, in the preparation and washing process, some EVAM adhered to the surface of SiO₂ may detach, leading to a significant increase in the inorganic component proportion in the EVAM/SiO₂ composite material. In contrast, the weight loss for the EVAM-g-NSiO₂ system is 99.06%, indicating that through chemical grafting, EVAM is fully coated on the surface of NSiO₂ in the EVAM-g-NSiO₂ composite system. This ensures good stability, reducing the loss of EVAM during the preparation process and enhancing the effectiveness of

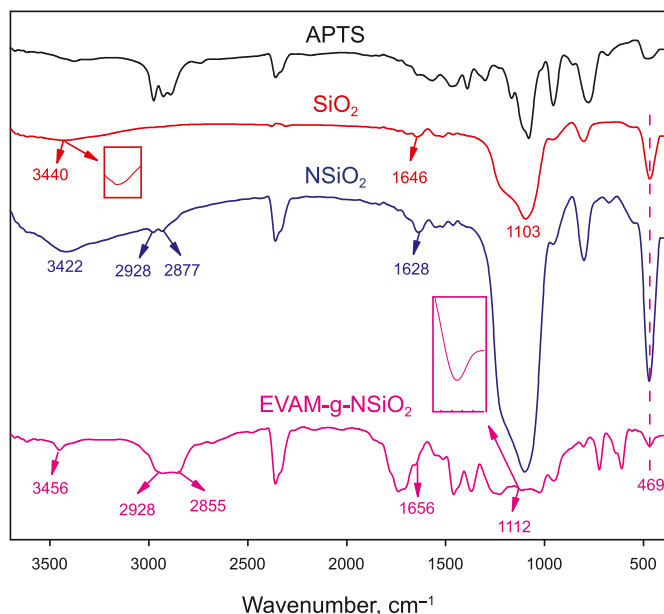


Fig. 5. FTIR of APTS, SiO₂, NSiO₂ and EVAM-g-NSiO₂.

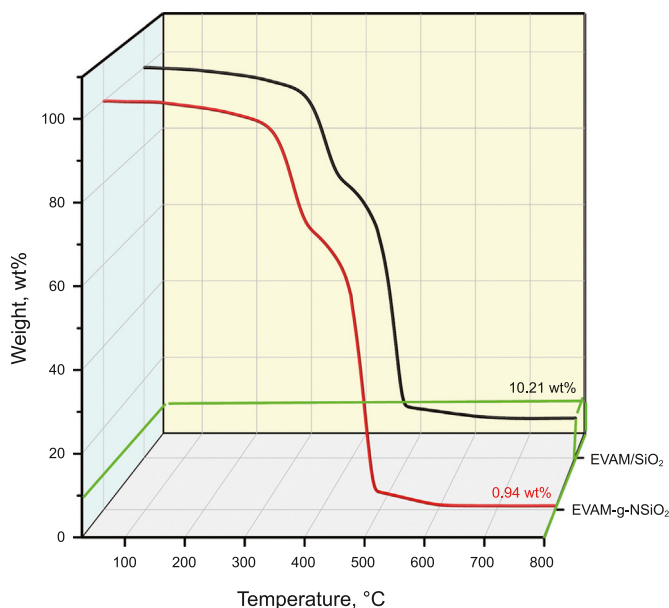


Fig. 6. TGA curves of EVAM/SiO₂ and EVAM-g-NSiO₂.

the nanocomposite system on crude oil. As shown in the graph, the residual mass after the pyrolysis of EVAM/SiO₂ and EVAM-g-NSiO₂ is 10.21% and 0.94%, respectively.

3.4. Pour point

As shown in Fig. 7, the pour point reduction of the model waxy oil shows a continuous increase with the escalating dosage of the PPD, ultimately reaching a stabilized state. The EVAM-g-NSiO₂ nanocomposite PPD showed better pour point reduction at different amounts of doping compared to EVA, EVAM and EVAM/SiO₂. At an additive dosage of 100 mg/kg, the EVAM-g-NSiO₂ nanocomposite PPD lowered the pour point of model waxy oil by 7 °C, whereas oil samples with the same dosage of EVA, EVAM, and EVAM/SiO₂ only reduced the pour point by 1, 4, and 3 °C, respectively. As the dosage increases, the pour point reduction of each oil sample is further enhanced. The EVAM-g-NSiO₂ nanocomposite PPD exhibits optimal pour point reduction when added at a dosage of 500 mg/kg, resulting in the pour point of the model waxy oil being lowered to 12 °C. Compared to oil samples added with the same dosage of EVA, EVAM, and EVAM/SiO₂, the pour point is further reduced by 11, 8, and 9 °C, respectively. Subsequently, rheological experiments were conducted at the optimal dosage (500 mg/kg).

3.5. Rheological properties

As shown in Fig. 8(a), the oil samples doped with different concentrations of EVAM-g-NSiO₂ nanocomposite PPDs exhibited good fluidity at low temperatures. The viscosity of the model waxy oil, undoped with EVAM-g-NSiO₂, starts to increase dramatically when the temperature is lowered to 36 °C, and the viscosity reaches as high as 2399 mPa·s at 32 °C. In contrast, the model waxy oil with only a low concentration (100 mg/kg) of EVAM-g-NSiO₂ starts to increase in viscosity at 32 °C, and it takes a temperature decrease to 27 °C for the viscosity to reach 2399 mPa·s. Notably, the oil sample doped with 500 mg/kg EVAM-g-NSiO₂ maintains a viscosity of a mere 2.4 mPa·s at 32 °C, reflecting an impressive viscosity reduction rate of 99.9%. Moreover, at 20 °C, the viscosity of the oil sample is merely 251.9 mPa·s.

Fig. 8(b) presents the viscosity-temperature curves of oil

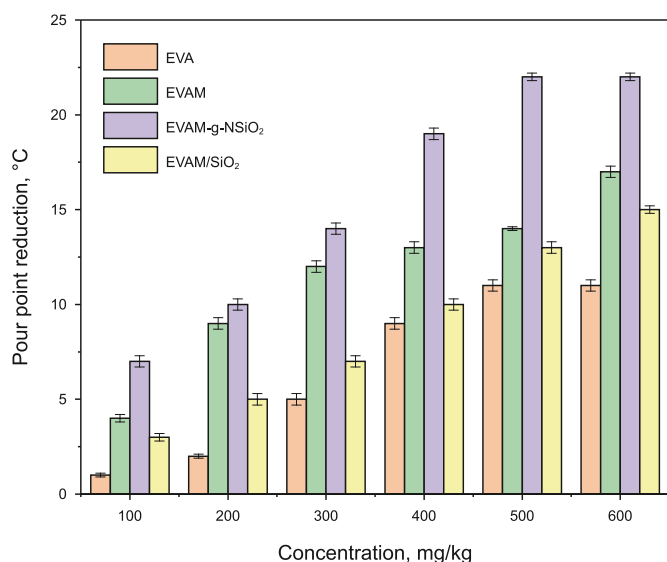


Fig. 7. Pour point reduction of model waxy oil with different concentrations PPDs.

samples doped with 500 mg/kg of various PPDs. Notably, the introduction of each PPD enhances the low-temperature flow characteristics of the model waxy oil. Compared to EVA, EVAM, and EVAM/SiO₂, the viscosity of the oil samples doped with EVAM-g-NSiO₂ nanocomposite PPD started to increase sharply only after 25 °C. This phenomenon may be attributed to the heightened stability of SiO₂ post-organic modification and EVAM grafting. EVAM-g-NSiO₂ can act as a crystalline nucleus, modifying the morphology of wax crystals, resulting in denser crystals and, consequently, a delayed viscosity increase. It is worth noting that at low temperatures, the viscosity of the oil samples doped with EVAM-g-NSiO₂ nanocomposite PPD exhibits a smoother trend compared to the oil samples doped with EVA, EVAM, and EVAM/SiO₂ PPDs. In summary, doped with 500 mg/kg EVAM-g-NSiO₂ nanocomposite PPD effectively improves the low-temperature flowability of the model waxy oil, consistent with the results of the pour point tests.

3.6. Micro-observation of the undoped/doped model waxy oil

Fig. 9 shows the microstructure of the undoped/doped with PPDs model waxy oil at 20 °C. As shown in Fig. 9(a), the wax crystals in the pure model waxy oil are in large blocks, presenting both sheet-like and elongated needle-like shapes. The quantity is abundant and loosely arranged, with wax crystal layers stacking and interconnecting, enveloping the liquid oil in clusters, ultimately resulting in the loss of flowability in the model waxy oil. In Fig. 9(b), doped with 500 mg/kg EVA, the wax crystals adopt a rod-shaped morphology with reduced dimensions; however, there is no substantial decrease in wax precipitation. The wax crystal morphology of the model waxy oil doped with 500 mg/kg EVAM (Fig. 9(c)) was significantly changed. The wax crystals gradually cluster, resembling the growth of “dandelions” and their dimensions decrease. In addition to alterations in wax crystal morphology, there is a significant reduction in the overall quantity of wax crystals. As shown in Fig. 9(d), the wax crystal morphology changed significantly after doped 500 mg/kg EVAM/SiO₂, but the wax precipitation increased slightly. The observed results are attributed to the poor compatibility between EVAM and SiO₂ after physical blending, causing partial separation and weakening the synergistic effect. Additionally, a portion of EVAM encapsulated the SiO₂, failing to disperse wax crystals effectively, resulting in irregular wax crystal formation and worsening the flow of the model waxy oil at low temperatures. The morphology of wax crystals, doped with 500 mg/kg EVAM-g-NSiO₂ nanocomposite PPD (Fig. 9(e)), underwent significant changes. The wax crystals display heightened compactness, featuring a more regular and rounded shape. The precipitation of wax crystals is effectively managed, leading to increased gaps between them. This contributes to the enhanced low-temperature flowability of the oil sample. Comparing Fig. 9(d) with Fig. 9(e), it can be observed that there are more wax crystals in Fig. 9(d), and their sizes vary, with irregular shapes. This is because the stability of the nanocomposite PPDs obtained by physical blending is poor. At the same time, the nanoparticle content enclosed in the nanocomposite PPDs obtained by physical blending is also higher, leading to more nucleation sites, thus increasing wax crystal precipitation.

3.7. Discussion on the mechanism of EVAM-g-NSiO₂ PPD

As shown in Fig. 10, the non-polar segment of the EVAM PPD undergoes eutectic precipitation with wax crystals in the model waxy oil, while the polar segment influences the growth direction of the wax crystals, resulting in their adsorption on the PPD molecules. On the other hand, the EVAM-g-NSiO₂ nanocomposite PPD serves as the crystallization nucleus for wax crystals, altering their

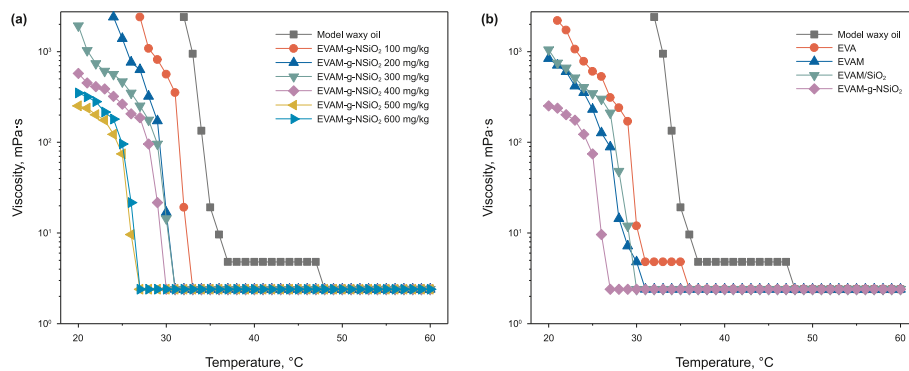


Fig. 8. Viscosity-Temperature curves of oil samples: (a) doped with different concentrations of EVAM-g-NSiO₂; (b) undoped and doped with 500 mg/kg PPDs.

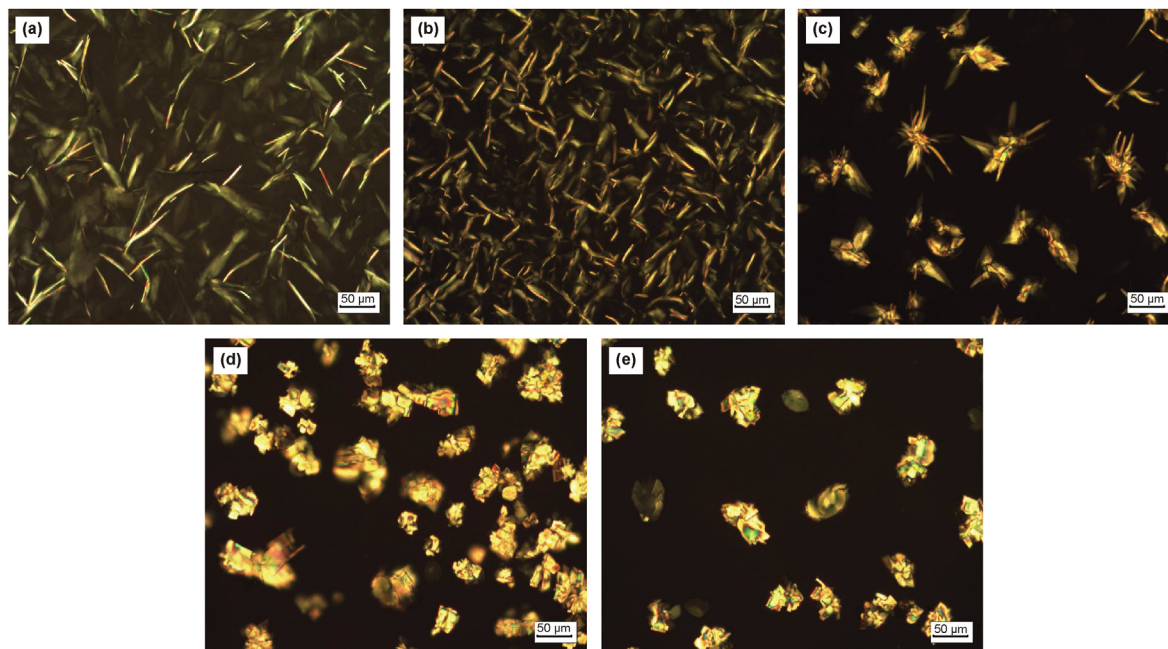


Fig. 9. Microscopic images of model waxy oil with and undoped and doped with PPDs at 20 °C: (a) undoped; doped with (b) 500 mg/kg EVA; (c) 500 mg/kg EVAM; (d) 500 mg/kg EVAM/SiO₂; (e) 500 mg/kg EVAM-g-NSiO₂.

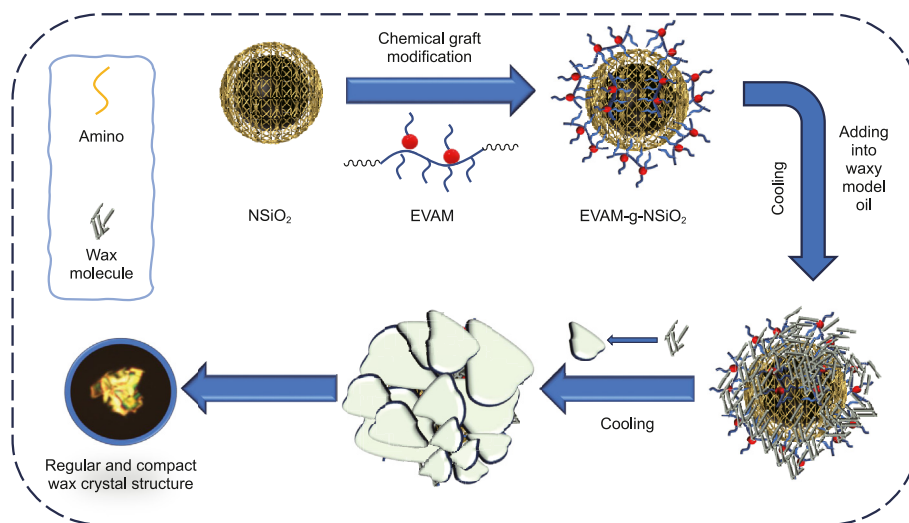


Fig. 10. Possible mechanism of EVAM-g-NSiO₂ nanocomposite PPD for improving the flowability of model waxy oil.

morphology and leading to the formation of spherical wax crystals. Simultaneously, the EVAM-g-NSiO₂ nanocomposite PPD functions as a template for wax precipitation, resulting in larger and denser wax morphologies (refer to Fig. 10). Large wax crystal size (resulting in a reduced solid-liquid interface area) and a dense structure (leading to less oil occlusion) are unfavorable for the formation of a robust gel network structure.

4. Conclusion

This paper obtained NSiO₂ through organic modification of inorganic nano silicon dioxide, and then successfully prepared EVAM-g-NSiO₂ nano composite PPD by chemical grafting method with the mass ratio of NSiO₂ to EVAM being 1:100. EVAM molecules were observed to significantly augment the lipophilicity of the nanoparticles. Additionally, a robust interaction between EVAM molecules and NSiO₂ was identified, resulting in a challenging desorption process from the surface of the organic nanoparticles. The impact of the EVAM-g-NSiO₂ nanocomposite PPD on the rheological properties and wax crystallization behavior of model waxy oil was investigated. The results indicated that the nanocomposite PPD particles served as templates for wax precipitation, resulting in larger and denser wax forms. The large size of wax crystals (reducing the wax crystal/oil interface) and dense structure (reducing liquid oil trapped in the wax crystal structure) were unfavorable for the formation of a network structure, contributing to the improved rheological performance of the model waxy oil.

CRediT authorship contribution statement

Yi-Hai Yang: Writing – review & editing, Writing – original draft, Visualization, Validation, Methodology, Investigation, Formal analysis, Data curation. **Li-Na Zhang:** Validation, Data curation. **Zheng-Nan Sun:** Supervision, Methodology. **Ming-Xing Bai:** Supervision, Funding acquisition. **Guo-Lin Jing:** Supervision, Resources, Funding acquisition. **Yang Liu:** Validation, Formal analysis. **Xiao-Yan Liu:** Supervision, Funding acquisition.

Declaration of competing interest

The authors declare that they have no known competing financial interests or personal relationships that could have appeared to influence the work reported in this paper.

Acknowledgments

This work was supported by the National Natural Science Foundation of China (No. 52076036). This work was supported by the National Natural Science Foundation of China (No. 52174020).

Appendix A. Supplementary data

Supplementary data to this article can be found online at <https://doi.org/10.1016/j.petsci.2024.06.012>.

References

- Aiyejina, A., Chakrabarti, D.P., Pilgrim, A., et al., 2011. Wax formation in oil pipelines: a critical review. *Int. J. Multiphase Flow*. 37 (7), 671–694. <https://doi.org/10.1016/j.ijmultiphaseflow.2011.02.007>.
- Al-Sabagh, A.M., Khidr, T.T., Moustafa, H.Y., et al., 2017. Synergistic effect between surfactants and polyacrylates-maleicanhydride copolymers to improve the flow properties of waxy crude oil. *J. Dispersion Sci. Technol.* 38 (7), 1055–1062. <https://doi.org/10.1080/01932691.2016.1219952>.
- Alves, B.F., Silva, B.K.M., Silva, C.A., et al., 2023. Preparation and evaluation of polymeric nanocomposites based on EVA/montmorillonite, EVA/palygorskite and EVA/halloysite as pour point depressants and flow improvers of waxy

- systems. *Fuel* 333 (Part 2), 126540. <https://doi.org/10.1016/j.fuel.2022.126540>.
- Azevedo, L.F.A., Teixeira, A.M., 2003. A critical review of the modeling of wax deposition mechanisms. *Petrol. Sci. Technol.* 21 (3–4), 393–408. <https://doi.org/10.1081/LFT-120018528>.
- Elbanna, S.A., Abd El Rhman, A.M.M., Al-Hussaini, A.S., et al., 2017. Synthesis and characterization of polymeric additives based on α -Olefin as pour point depressant for Egyptian waxy crude oil. *Petrol. Sci. Technol.* 35 (10), 1047–1054. <https://doi.org/10.1080/10916466.2017.1307852>.
- Fang, L., Zhang, X., Ma, J., et al., 2012. Investigation into a pour point depressant for shengli crude oil. *Ind. Eng. Chem. Res.* 51 (36), 11605–11612. <https://doi.org/10.1021/ie301018r>.
- Ghosh, P., Das, M., 2014. Study of the influence of some polymeric additives as viscosity index improvers and pour point depressants-Synthesis and characterization. *J. Petrol. Sci. Eng.* 119, 79–84. <https://doi.org/10.1016/j.petrol.2014.04.014>.
- Ghosh, P., Dey, K., Upadhyay, M., et al., 2017. Multifunctional biodegradable lube oil additives: synthesis, characterization, and performance evaluation. *Petrol. Sci. Technol.* 35 (1), 66–71. <https://doi.org/10.1080/10916466.2016.1248770>.
- Jia, X.L., Fu, M.M., Xing, X.Y., et al., 2022. Submicron carbon-based hybrid nanopour-point depressant with outstanding pour point depressant and excellent viscosity depressant. *Arab. J. Chem.* 15 (10), 104157. <https://doi.org/10.1016/j.arabjc.2022.104157>.
- Jing, G.L., Sun, Z.N., Tu, Z.Y., et al., 2017. Influence of different vinyl acetate contents on the properties of the copolymer of ethylene and vinyl acetate/modified nano-SiO₂ composite pour-point depressant. *Energy Fuel*. 31 (6), 5854–5859. <https://doi.org/10.1021/acs.energyfuels.7b00189>.
- Liu, Y., Sun, Z.N., Ji, S.Z., et al., 2023. Effect of nanocomposite pour point depressant EVAL/CNT on flow properties of waxy crude oil. *Petrol. Sci.* 20 (6), 3807–3818. <https://doi.org/10.1016/j.petsci.2023.05.016>.
- Liu, Y., Sun, Z.N., Jing, G.L., et al., 2021. Synthesis of chemical grafting pour point depressant EVAL-GO and its effect on the rheological properties of Daqing crude oil. *Fuel Process. Technol.* 223, 107000. <https://doi.org/10.1016/j.fuproc.2021.107000>.
- Norrman, J., Solberg, A., Sjöblom, J., et al., 2016. Nanoparticles for waxy crudes: effect of polymer coverage and the effect on wax crystallization. *Energy Fuel*. 30 (6), 5108–5114. <https://doi.org/10.1021/acs.energyfuels.6b00286>.
- Paul, D.R., Robeson, L.M., 2008. Polymer nanotechnology: nanocomposites. *Polymer* 49 (15), 3187–3204. <https://doi.org/10.1016/j.polymer.2008.04.017>.
- Pedersen, K.S., Rønningsen, H.P., 2003. Influence of wax inhibitors on wax appearance temperature, pour point, and viscosity of waxy crude oils. *Energy Fuel*. 17 (2), 321–328. <https://doi.org/10.1021/ef020142>.
- Ruwoldt, J., Simon, S., Norrman, J., et al., 2017. Wax-inhibitor interactions studied by isothermal titration calorimetry and effect of wax inhibitor on wax crystallization. *Energy Fuel*. 31 (7), 6838–6847. <https://doi.org/10.1021/acs.energyfuels.7b00749>.
- Schmidt, D., Shah, D., Giannelis, E.P., 2002. New advances in polymer/layered silicate nanocomposites. *Curr. Opin. Solid State Mater. Sci.* 6 (3), 205–212. [https://doi.org/10.1016/S1359-0286\(02\)00049-9](https://doi.org/10.1016/S1359-0286(02)00049-9).
- Sharma, R., Deka, B., Mahto, V., et al., 2019a. Investigation into the flow assurance of waxy crude oil by application of graphene-based novel nanocomposite pour point depressants. *Energy Fuel*. 33 (12), 12330–12345. <https://doi.org/10.1021/acs.energyfuels.9b03124>.
- Sharma, R., Mahto, V., Vuthaluru, H., 2019b. Synthesis of PMMA/modified graphene oxide nanocomposite pour point depressant and its effect on the flow properties of Indian waxy crude oil. *Fuel* 235, 1245–1259. <https://doi.org/10.1016/j.fuel.2018.08.125>.
- Silviya, E.K., Unnikrishnan, G., Varghese, S., et al., 2012. Thermal and mechanical characterization of EVA/banana fiber-derived cellulose composites. *J. Appl. Polym. Sci.* 125 (1), 786–792. <https://doi.org/10.1002/app.35140>.
- Steckel, L., Nunes, R.C.P., Rocha, P.C.S., et al., 2022. Pour point depressant: identification of critical wax content and model system to estimate performance in crude oil. *Fuel* 307, 121853. <https://doi.org/10.1016/j.fuel.2021.121853>.
- Sun, Z.N., Jing, G.L., Tu, Z.Y., 2018. Effect of modified nano-silica/EVA on flow behavior and wax crystallization of model oils with different wax contents. *J. Dispersion Sci. Technol.* 39 (1), 71–76. <https://doi.org/10.1080/01932691.2017.1295869>.
- Umoruddin, N.E.S., Rosdi, M.R.H., Ariffin, A., 2019. Mixed surfactant enabled EVA emulsion for PPD applications. *J. Dispersion Sci. Technol.* 40 (3), 361–368. <https://doi.org/10.1080/01932691.2018.1469413>.
- Valinejad, R., Nazar, A., 2013. An experimental design approach for investigating the effects of operating factors on the wax deposition in pipelines. *Fuel* 106, 843–850. <https://doi.org/10.1016/j.fuel.2012.11.080>.
- Wei, B., 2015. Recent advances on mitigating wax problem using polymeric wax crystal modifier. *J. Pet. Explor. Prod. Technol.* 5 (4), 391–401. <https://doi.org/10.1007/s13202-014-0146-6>.
- Yang, F., Paso, K., Norrman, J., et al., 2015a. Hydrophilic nanoparticles facilitate wax inhibition. *Energy Fuel*. 29 (3), 1368–1374. <https://doi.org/10.1021/ef502392g>.
- Yang, F., Yao, B., Li, C., et al., 2017. Performance improvement of the ethylene-vinyl acetate copolymer (EVA) pour point depressant by small dosages of the poly-methylsilsesquioxane (PMSQ) microsphere: an experimental study. *Fuel* 207, 204–213. <https://doi.org/10.1016/j.fuel.2017.06.083>.
- Yang, F., Zhao, Y., Sjöblom, J., et al., 2015b. Polymeric wax inhibitors and pour point depressants for waxy crude oils: a critical review. *J. Dispersion Sci. Technol.* 36 (2), 213–225. <https://doi.org/10.1080/01932691.2014.901917>.
- Yang, Y.H., Sun, Z.N., Jing, G.L., et al., 2023. Study on the effect of polyoctadecyl

- acrylate on daqing waxy oil. *Recent Innovat. Chem. Eng.* 16 (2), 147–156. <https://doi.org/10.2174/2405520416666230614122518>.
- Yao, B., Li, C., Yang, F., et al., 2016a. Organically modified nano-clay facilitates pour point depressing activity of polyoctadecylacrylate. *Fuel* 166, 96–105. <https://doi.org/10.1016/j.fuel.2015.10.114>.
- Yao, B., Li, C.X., Yang, F., et al., 2016b. Structural properties of gelled Changqing waxy crude oil benefitted with nanocomposite pour point depressant. *Fuel* 184, 544–554. <https://doi.org/10.1016/j.fuel.2016.07.056>.
- Yao, B., Li, C.X., Zhang, X.P., et al., 2018. Performance improvement of the ethylene-vinyl acetate copolymer (EVA) pour point depressant by small dosage of the amino-functionalized polymethylsilsesquioxane (PAMSQ) microsphere. *Fuel* 220 (1), 167–176. <https://doi.org/10.1016/j.fuel.2018.01.032>.
- Zhang, F., Liu, J., Zhu, X., et al., 2020. Performance improvement of the benzyl methacrylate-methacrylate copolymers pour point depressant by hybrid with nano-silica for diesel fuels. *Energ. Source. Part. A.* 1–9. <https://doi.org/10.1080/15567036.2020.1751746>.
- Zhao, Z.C., Xue, Y., Xu, G.W., et al., 2017. Effect of the nano-hybrid pour point depressants on the cold flow properties of diesel fuel. *Fuel* 193, 65–71. <https://doi.org/10.1016/j.fuel.2016.12.020>.